Available online at www.sciencedirect.com
ScienceDirect
Biochimica et Biophysica Acta 1767 (2007) 197–203
Biochimica et Biophysica Acta
BBA
www.elsevier.com/locate/bbabio

Protons bound to the Mn cluster in photosystem II oxygen evolving complex detected by proton matrix ENDOR

Hiroiku Yamada, Hiroyuki Mino *, Shigeru Itoh

Division of Material Science (Physics), Graduate school of Science, Nagoya University, Furocho, Chikusa, Nagoya, 464-8602, Japan

Received 3 June 2006; received in revised form 1 February 2007; accepted 2 February 2007
Available online 9 February 2007

Abstract

Protons in the vicinity of the oxygen-evolving manganese cluster in photosystem II were studied by proton matrix ENDOR. Six pairs of proton ENDOR signals were detected in both the S_0 and S_2 states of the Mn-cluster. Two pairs of signals that show hyperfine constants of 2.3/2.2 and 4.0 MHz, respectively, disappeared after D_2O incubation in both states. The signals with 2.3/2.2 MHz hyperfine constants in S_0 and S_2 state multiline disappeared after 3 h of D_2O incubation in the S_0 and S_1 states, respectively. The signal with 4.0 MHz hyperfine constants in S_0 state multiline disappeared after 3 h of D_2O incubation in the S_0 state, while the similar signal in S_2 state multiline disappeared only after 24 h of D_2O incubation in the S_1 state. The different proton exchange rates seem to be ascribable to the change in affinities of water molecules to the variation in oxidation state of the Mn cluster during the water oxidation cycle. Based on the point dipole approximation, the distances between the center of electronic spin of the Mn cluster and the exchangeable protons were estimated to be 3.3/3.2 and 2.7 Å, respectively. These short distances suggest the protons belong to the water molecules ligated to the manganese cluster. We propose a model for the binding of water to the manganese cluster based on these results.

Keywords: EPR; ESR; ENDOR; Mn-cluster; Oxygen evolution; Photosystem II

Photosynthetic O_2 evolution in green plants and cyanobacteria is catalyzed by the oxygen-evolving complex (OEC) located on the lumenal side of D1 protein in the membrane-bound photosystem (PS) II reaction center protein complex [1–3]. OEC contains four Mn ions and Cl^- and Ca^{2+} cofactors. X-ray crystallographic analyses have revealed the 3D structure of PS II at 3.2–3.8 Å resolution [4–7], although the precise geometric and electronic structure of the manganese cluster in OEC is not yet clear. Recently, the structure at 3.0 Å resolution has also been reported [8]. In light-driven water oxidation in PS II, two water molecules are oxidized to yield an oxygen molecule through a cycle of five distinct redox states labeled S_n ($n=0$–4). The S_1 state is most stable in darkness and each S_n state advances to S_{n+1} by the single photon reaction in PS II. As the highest oxidation state S_4 is attained by the successive photoreactions, S_4 spontaneously converts to S_0, which is the lowest oxidation state, with the release of an oxygen molecule [1,2].

Since the discovery of the multiline signal of the manganese cluster in the S_2 state [9], EPR spectroscopy has been extensively applied to the study of the OEC. The S_2 state multiline signal is centered at $g=2$ expanded over approximately 1600 G. The signal shows 19–21 hyperfine lines spaced by 85–90 G from each other and is ascribed to the $S=1/2$ ground state. It has been suggested that the Mn cluster is a multinuclear complex in the S_2 state that includes a Mn (III)–Mn (IV) pair [9]. On the other hand, simulation studies have indicated the oxidation state of the four Mn ions in the S_2 state to be Mn_4(III,IV,IV,IV) [10–13] or Mn_4(III,III,III,IV) [10]. ^{55}Mn pulsed ENDOR measurements suggested the Mn_4(III,IV,IV,IV) model to be more probable [14,15]. Recently, a new multiline signal in the S_0 state has been discovered and shown to be composed of at least 26 peaks ascribable to the $S=1/2$ ground state in the presence of methanol [16,17]. ^{55}Mn pulsed ENDOR experiments at Q-band have revealed that the hyperfine constants of the individual Mn ions

Abbreviations: EIE, ENDOR-induced EPR; ENDOR, electron nuclear double resonance; EPR, electron paramagnetic resonance; ESE, electron spin echo; MES, 2-morpholinoethanesulfonic acid; OEC, oxygen-evolving complex; PS II, photosystem II; Y_D, Tyr161 of the D2 subunit in PS II

* Corresponding author. Tel.: +81 52 789 2883; fax: +81 52 789 2883.
E-mail address: mino@bio.phys.nagoya-u.ac.jp (H. Mino).

0005-2728/$ - see front matter © 2007 Elsevier B.V. All rights reserved.
doi:10.1016/j.bbabio.2007.02.001

are very similar in the S_0 and S_2 states. An ENDOR study estimated Mn_4(III,III,III,IV) for the S_0 state and Mn_4 (III,IV,IV, IV) for the S_2 state [15].

Mass spectrometric measurements employing rapid (ms) $H_2{}^{16}O/H_2{}^{18}O$ exchange demonstrate that one substrate water molecule is bound to the OEC throughout the Kok cycle and exchanges with an S_n state dependent half-time in the order of seconds. The second, faster exchanging substrate water was detected in the S_2 and S_3 states [18–20]. It is currently unclear whether (i) the faster exchanging substrate water is also bound in the S_0 and S_1 states and (ii) in which protonation state and geometry the two substrate water molecules are bound to the OEC (for review see Hillier and Messinger [21]). Other techniques applied to study water or proton binding include FTIR [22], NMR [23–26] and EPR/ENDOR.

ENDOR has been a valuable method for investigating the coordination state of water molecules to the Mn cluster. Kawamori et al. detected 6 pairs of ENDOR lines in the S_2 multiline signal, and have estimated the distances of protons from the Mn-cluster at 2.7–6.0 Å based on the point dipole approximation [27]. Tang et al. [28] and Fiege et al. [29] have also investigated the S_2 state by CW ENDOR and detected exchangeable protons that might be ligated directly to the Mn cluster. ESEEM studies suggested the contributions of two or three water protons to the signals in the S_2 [30] and S_0 state [31]. These results suggested that the water molecules bind directly to the Mn cluster in the S_0 and S_2 states [19,20] in agreement with the mass spectroscopy results [18–20,22].

In this report, we investigate the proton exchange rate in the S_0 and S_2 states using the proton matrix ENDOR method.

1. Materials and methods

1.1. Sample preparation

Oxygen-evolving PS II membranes were prepared from spinach according to the method previously described [32] with a slight modification [33]. The obtained PS II membranes were suspended in a medium containing 0.4 M sucrose, 20 mM NaCl, 1 mM EDTA, 50 mM Mes/NaOH buffer at pH 6.5 (medium A) and stored in liquid N_2 until use.

"S_1-enriched PS II membranes" were prepared by dark adaptation of the PS II membranes for 2 h at 273 K after the short pre-illumination as reported previously [34]. Messinger et al. have succeeded in populating the S_0 state by reduction of $Y_D^\bullet$ using trifluoromethoxy carbonylcyanide phenylhydrazone [35]. In the present study, sodium ascorbate was used for reduction of $Y_D^\bullet$. For the preparation of "S_0-enriched membranes", the S_1-enriched membranes were resuspended in medium A supplemented with 100 mM sodium ascorbate to give a final concentration of 2 mg Chl/ml, and then the membranes were incubated overnight in darkness at 273 K in order to reduce $Y_D^\bullet$ radical completely. The dark-incubated membranes were resuspended in the same medium containing 1 mM phenyl-*p*-benzoquinone and 1 mM potassium ferricyanide to give a final concentration of 1 mg Chl/ml. The membranes were transferred into a Petri dish, and illuminated with three successive flashes of Nd-YAG laser (200 mJ/pulse, 532 nm, at 1 Hz) at 273 K at the saturating intensity to populate the S_0 state efficiently. The membranes were then washed with medium A containing 1.5% methanol, and dark-adapted at 273 K. Some centers in the S_2 or S_3 states produced by double- and miss- hits, were relaxed into the S_1 state by dark incubation. Although some Y_D centers were reoxidized by back reactions, absence of $Y_D^\bullet$ inhibited the S_0 to S_1 state transition, and as a result, the stable S_0 state was populated. The S_0 and S_1-enriched membranes were centrifuged, and then, the concentrated membranes were directly pushed into suprasil quartz EPR tubes with a syringe (Terumo, Tokyo) through a 30-cm needle (home-made) to give a final concentration of more than 15 mg Chl/ml, and stored at 77 K until use. The S_2 state was formed as follows; the S_1-enriched membranes were resuspended in medium A containing 50% ethylene glycol and 1.5% methanol in the dark, and then illuminated for 5 min at 200 K.

Deuterated methanol (Merck), deuterated ethylene glycol (Icon. Inc.), and sucrose, solubilized and incubated in D_2O (Merck), were used for the deuterium-exchange experiments. The membranes in the S_0 and S_1 states were incubated for 3 or 24 h in the D_2O exchanged medium, as shown schematically in Fig. 1.

1.2. EPR measurements

EPR measurements were performed using a Bruker ESP-300E ESR spectrometer with a gas flow temperature control system (CF935, Oxford Instruments, Oxford, GB). EPR signals were measured with a standard resonator (ER4102). ENDOR signals were detected with a 12.5 kHz modulation frequency. 300 mW radio wave from an RF power amplifier (A-500, ENI) was supplied to 12 lines of ENDOR coils that were placed parallel to the cylindrical axis of the TE_{011} cavity and terminated with a 50 Ω dummy load [27].

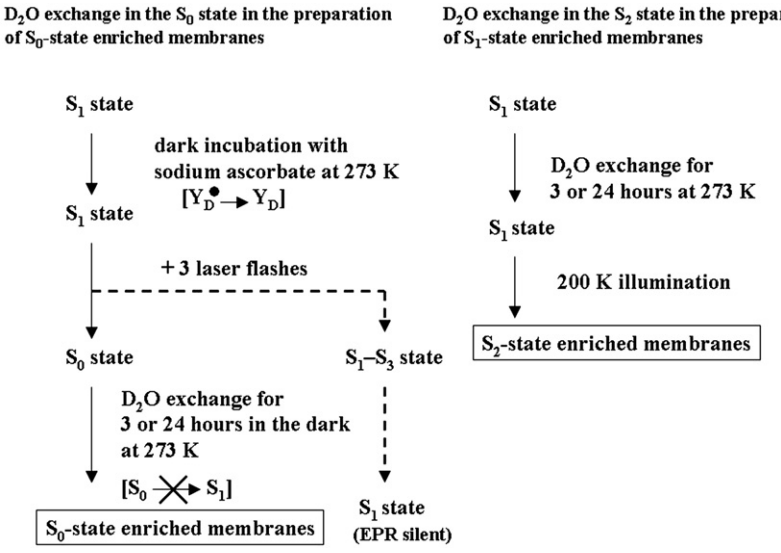

Fig. 1. Block diagrams of the deuterium exchange in the S_0 and S_1 states for the S_0 and S_2 state-enriched PS II membranes, respectively.

2. Results

EPR spectra of the spinach PS II membranes, enriched for the S_0, S_1 or S_2 state as described in Materials and methods, were measured at cryogenic temperatures. Fig. 2 shows the S_0-minus-S_1 (A) and the S_2-minus-S_1 (B) difference EPR spectra obtained at 4.5 K. The spectrum obtained in the S_1 state, which contains signals of cytochrome *b*559 and background signal, was used as the base line. The signal intensities were adjusted at the intensity of the rhombic Fe signal. The spectrum measured in the S_0-enriched membrane (trace A) showed a 1800 G width having at least 22 peaks with an average splitting width of 90 G, which is a typical S_0 state multiline signal [16,35,36]. Trace B shows a typical S_2 multiline signal, comprising at least 17 peaks with a spectral width of 1600 G [9]. From the amplitude of the S_2 multiline signal detected after the 200 K illumination of the S_0-enriched membranes, we can estimate that more than 50% of the PS II OEC are populated in the S_0 state in the "S_0-enriched membranes", and the rest are populated in the S_1 state, which is EPR silent in conventional mode EPR.

Fig. 3 shows the ENDOR spectra obtained in the membranes incubated in the ordinary H_2O medium (traces A and D), and those incubated in D_2O medium for 3 h (traces B and E) and 24 h (traces C and F) in the S_0 state (traces A–C) or S_2 state (traces D–F), respectively. The shapes and intensities of both S_0 and S_2 multiline signals did not change after 3 and 24 h incubation (data not shown). For the measurements in the S_0 and S_2 states, magnetic fields were fixed at positions 50 G higher or lower than that of $Y_D^{\bullet}$ radical, respectively. The ENDOR intensities were normalized by multiline intensities. The spectrum in the S_1-state was obtained separately (dotted lines in Fig. 3), and was subtracted from the spectra in the S_0 and S_2 states as a baseline signal.

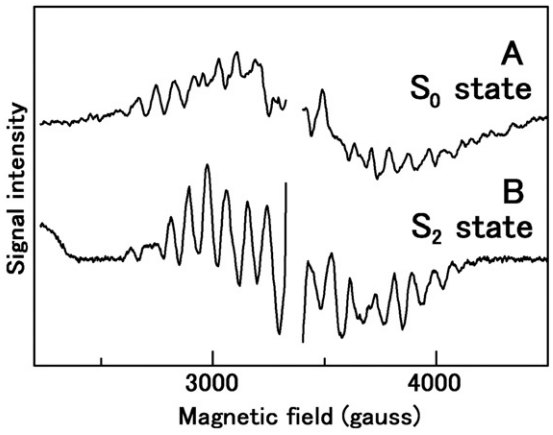

Fig. 2. EPR spectra of S_0 (trace A) and S_2 state (trace B). The spectra in S_0, S_1 and S_2 state were measured in the PS II membranes enriched for these three states as described in Materials and methods. The S_0 and S_2 state spectra in traces A and B are obtained by subtracting the spectra of the S_1 state measured under the same conditions. Experimental conditions for the EPR measurements: microwave frequency, 9.35 GHz; microwave power, 0.8 mW for S_2 state and 1.5 mW for S_0 state; modulation amplitude, 5.6 gauss; temperature, 4.5 K for S_2 state and 4.0 K for S_0 state; scan time 42 s.

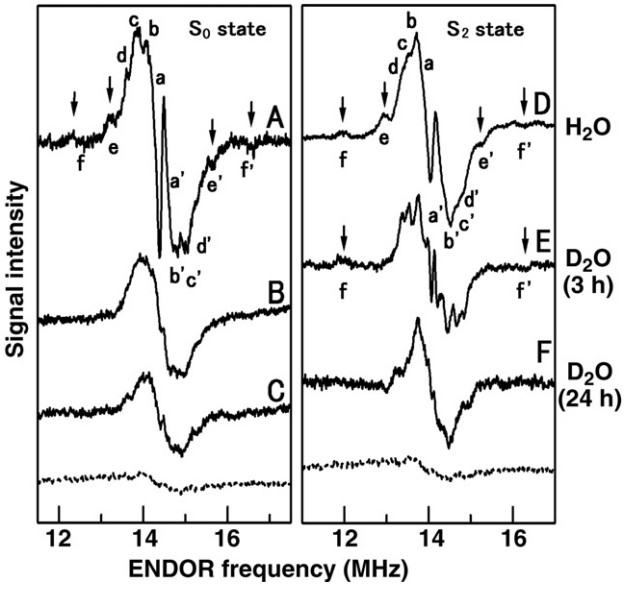

Fig. 3. ENDOR spectra of the S_0 (trace A–C) and S_2 (trace D–F) multiline signals. ENDOR spectra were measured in the S_0- and S_2-enriched PS II membranes either in the H_2O medium (trace A and D), or after incubation in the D_2O medium for 3 h (trace B and E) and 24 h (trace C and F). Dotted lines show the spectra in S_1 state. Experimental conditions: microwave frequency, 9.35 GHz; microwave power, 2.0 mW; RF power, 300 mW; FM depth, 100 kHz; temperature 4.5 K; magnetic field, 3266 gauss; scan time 20 min.

The broad featureless signal observed may arise from cytochrome *b*559. Six pairs of peaks labeled aa′–ff′ were present in the ENDOR spectra of both the S_0 and S_2 multiline signals (traces A and D). The separations of each pair, which give hyperfine constants, for ENDOR peaks of the S_0 (trace A) and S_2 (trace D) multiline signals were very similar, as listed in Table 1. Peaks ee′ and ff′ disappeared after the D_2O incubation (traces C and F), while the other peaks remained, confirming the results of the D_2O exchange in the S_2 state ENDOR previously reported [27].

Traces B and E show the ENDOR spectra of the S_0 and S_2 signals, respectively, after incubation in D_2O medium for 3 h. Note that the ee′ peaks and ff′ peaks disappeared from the S_0 state spectrum (trace B), but ff′ remained in the S_2 state spectrum (trace E). The differing behaviors of these two peaks indicate that they do not arise from the $A_{\perp}$ and $A_{//}$ axial symmetry components of the same proton [28,29].

The intensities in the central region of the ENDOR spectra (i.e. peaks aa′–dd′) also decreased by about 40 and 70%, respectively, after 24 h D_2O incubation. After 3 h incubation with D_2O, the S_0 ENDOR spectrum became featureless, while

Table 1
Hyperfine coupling constants in the S_0 and S_2 state spectra obtained by proton matrix ENDOR

	Peaks	aa′	bb′	cc′	dd′	ee′	ff′
S_0 state	$\Delta\nu$(MHz)	0.28	0.48	0.99	1.62	2.33	4.01
S_2 state	$\Delta\nu$(MHz)	0.43	0.69	1.10	1.38	2.19	4.00

The labels correspond to each set of ENDOR peaks denoted as aa′–ff′ measured in the S_0 and S_2 spectra.

some features remained in the S_2 ENDOR spectrum, with some loss of intensity in the center region.

ENDOR-induced EPR (EIE) is a useful method for the identification of the origin of ENDOR signals. Fig. 4 shows the EIE spectra measured for the S_0 (Panel A) and S_2 (Panel B) state ENDOR signals in H_2O medium (traces A and D in Fig. 3). The background spectrum has been subtracted in each case. EIE spectra were measured at ENDOR peak b for traces A and D in Fig. 4, peak e for traces B and E in Fig. 4, and peak f for traces C and F in Fig. 4, respectively. The sharp line around $g=2$ in each spectrum was ascribed to $Y_D^{\bullet}$ radicals, and the broad absorption shapes can be ascribed to the Mn cluster. We can easily extract the overlapping ENDOR signals of $Y_D^{\bullet}$ radical. Spectra A–C are about 1500 G wide and centered at around $g=1.93$ so that they can be ascribed to the S_0 multiline spectrum [15]. Spectra D–F are, on the other hand, centered at around $g=1.99$–2.00, confirming that they arise from the S_2 multiline signal. EIE analysis of the S_0 multiline signal agrees well with the result of field-swept ESE (electron spin echo) measured at Q-band that also indicated a center at a g value smaller than that of the S_2 spectrum [15].

Fig. 5 (left panel) shows ENDOR spectra in the D_2O-incubated PS II membranes to examine the effect of D_2O exchange during multi-turnover of S states under conditions with 273 K illumination. The experimental procedures are shown schematically in the right panel. The membranes were pre-illuminated for 1 min at 273 K in D_2O, and then incubated for 3 h in the dark (trace A). Both the ee′ and ff′ peaks disappeared in contrast to the incubation in the dark (trace D in Fig. 3). Trace B shows the spectrum of the membranes, incubated for 3 h in the D_2O medium in the dark without pre-illumination. Only the ee′ peaks disappeared. These results show that the protons giving rise to the ff′ peak were exchanged rapidly during cyclic turnovers of the S states, although these protons were exchanged slowly in the S_1 state.

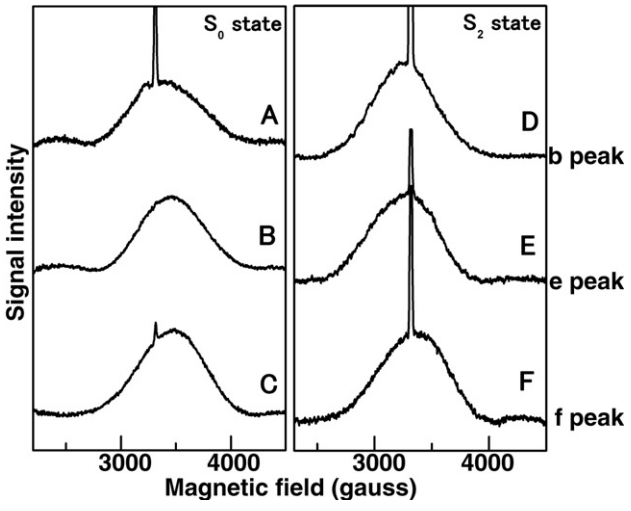

Fig. 4. ENDOR-induced EPR (EIE) spectra of S_0 (trace A–C) and S_2 (trace D–F) multiline signals. EIE spectra were measured at the ENDOR peak b for traces A and D, at peak e for traces B and E, and at peak f for traces C and F, respectively. Experimental conditions: microwave frequency, 9.35 GHz; microwave power, 4.0 mW; RF power, 300 mW; FM depth, 100 kHz; temperature 4.0 K; scan time 5 min.

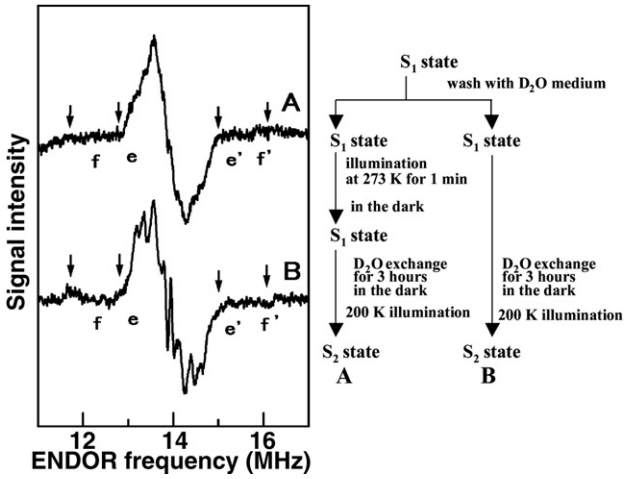

Fig. 5. ENDOR spectra of the S_2 multiline signals after D_2O incubation in S_1 state in D_2O medium (left panel), and the sample preparation procedure (right panel). Before illumination, the membranes were pre-illuminated for 1 min at 273 K in D_2O medium (trace A) or in H_2O medium (trace B) and dark-incubated for 3 h. D_2O exchange has been therefore performed in S_0–S_4 states (trace A) and S_1 state (trace B). Experimental conditions are the same as in Fig. 3.

3. Discussion

The determination of the proton matrix ENDOR signals of the S_0 and S_2 states confirm the ENDOR studies of the S_2 multiline signal reported previously [9,27,28]. The EIE measurements in this study further suggested that the signals originate from protons that are ligated to the Mn cluster.

The separation of peaks in the ENDOR spectrum is expressed as the sum of the dipolar interactions between protons and the spin density distributions on the Mn cluster. The proton ENDOR frequencies are given by

$$\upsilon^{\pm} = |\upsilon_H \pm a/2| \tag{1}$$

where υ_H and a are the Lamor frequency for proton and the hyperfine coupling constant, respectively. The hyperfine coupling constant consists of the Fermi contact interaction a_{iso} and the magnetic dipole interaction a_{aniso}. In the case of simple dipole model ($S=1/2$, $I=1/2$), ENDOR separation $\Delta\upsilon$ is expressed as the sum of the dipole interactions between proton and spin density distribution ρ, as

$$\Delta\upsilon = \Sigma_i \rho_i g_e \beta g_N \beta_N (1 - 3\cos^2\theta_i)/r_i^3 \tag{2}$$

where g_e and g_N are g-factors for electron and nuclei, respectively, β and β_N are Bohr magnetrons for electron and nuclei, respectively, r is the distance between the Mn cluster and the proton, and θ is the angle between the position vector and the direction of the magnetic field. In the case of randomly oriented molecules, the ENDOR spectrum has a maximum intensity with $A_\perp$ at $\theta=90°$. In this approximation, the space distribution of the Mn cluster was neglected.

ENDOR spectra of the S_0 and S_2 multiline signals are very similar, which is, however, rather unusual because the different spin centers generally should have different spin distribution values ρ. Kulik et al. have reported that the hyperfine constants obtained by ENDOR simulations of individual ^{55}Mn ions in the Mn cluster are very similar [15,37]. The similarities of the matrix ENDOR spectra in the S_0 and S_2 states, therefore, suggest similar proton arrangements at similar electronic spin distributions. Proton release has been reported in the S_0 to S_1 state transitions, suggesting structural modification of the Mn-cluster [38,39]. Some possible situations based on the results in the present study are: (1) the protons released during the S_0–S_1 state transition are not located in the vicinity of the manganese center; (2) the positions in which the protons are located are filled by other protons via a proton transfer pathway; (3) some proton might be undetectable in our ENDOR measurements due to their fast or slow nuclear relaxation rates.

The ee′ and ff′ peaks in the S_0-ENDOR signal, as well as the ee′ peak in the S_2 signal, disappeared after incubation in D_2O medium for 3 h. However, the ff′ peak in the S_2 signal did not disappear after 3 h incubation in D_2O medium. The sample tested in the S_2 state was incubated in D_2O medium in the S_1 state. Therefore, we can conclude that the affinity of the ff′ protons is stronger in the S_1 state than that in the S_0 state. Simple dipole approximation suggests the distances between the putative electronic spin center of the manganese cluster and the ee′ and ff′ protons to be 3.3 and 2.7 Å, respectively. These short distances indicate these protons to be almost in contact with the Mn cluster [27,29], if we assume both S_0 and S_2 states have effective spin $S=1/2$ [9–16]. Note that the distances are reached based on a simple estimation. Actually, the vicinity of the electron and proton may derive the Fermi contact interaction a_{iso}. The ff′ and ee′ protons may either belong to water molecules that are directly ligated to the Mn cluster or to the amino acid side-chains ligated to the Mn cluster.

The different exchange rates also suggest that the affinities of protons to the Mn cluster differ in the S_0 and S_1 states. On the other hand, the exchange rate of the ee′ proton was substantially faster than that of the ff′ proton and, in addition, the exchange rate of the ff′ proton in the S_1 state is very slow and dependent on the S-state, suggesting it arises from a functional proton. This indicates that the exchange of the ff′ proton is suppressed upon the transition of the S_0 to S_1 state and seems to support the proposal by Nugent et al. of channels specific for water access and proton release [40]. FTIR studies showed the enhanced reactions or movements of water molecules in the S_2 to S_3 and S_3 to S_0 transitions [22]. The higher accessibility of the water molecules in the S_0 state is consistent with our results. (^{16}O/^{18}O) isotope-exchange experiments, on the other hand, showed that exchange of water molecules in the S_2 and S_3 states occurs at two rates, suggesting the existence of two water binding sites both in the S_2 and S_3 states [20,41,42]. The slower exchangeable rate at 283 K was 10 s^{-1} in S_0 state and 0.02 s^{-1} in S_1 state, respectively, indicating that one substrate water is tightly bound in the S_1 state. The difference in exchange rates between S_0 and S_1 states agree with the behavior of ff′ protons measured in the present study. However, the exchange rate of 0.0055 s^{-1} in the S_1 state at 273 K, which also is the temperature used for D_2O incubation in our experiments, is far faster than that observed for the ff′ protons (half-times of minutes vs. hours). This appears to exclude that the ff′ signals originate from the protons of substrate water detected by mass spectrometric measurements. They therefore more likely represent protons from a Mn-ligand that is affected by the S_0 to S_1 transition. ^{2}H-ESEEM detected some proton signals with 0.3 and 0.6 MHz for deuterium (2 and 4 MHz for protons), suggesting relatively fast exchange rates [31]. We assume that the ee′ proton may be a good candidate as the proton bound to water detected in the (^{16}O/^{18}O) isotope-exchange experiment.

ENDOR signals measured within 2 MHz suggest distances longer than 4 Å (Table 1). These long distances are rather difficult to assign, because of the many protons expected to exist within such long distances. Ambient protons with Larmor frequency, which might be regulated by the local environment, have been detected by ^{2}H-ESEEM measurements [43]. Although we cannot exclude the possibility that the signals of substrate water are also included in the 2 MHz region, it seems most likely that substrate water molecules exist rather close to

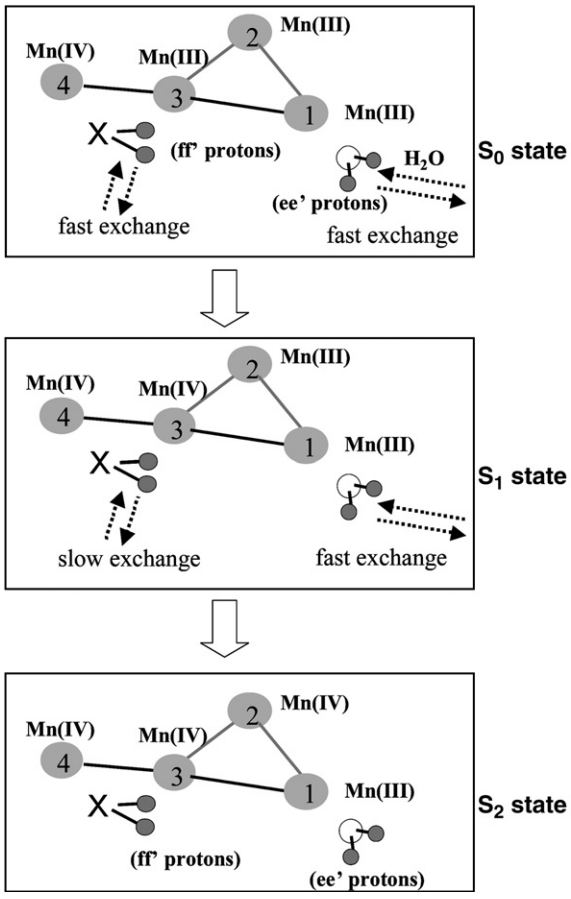

Fig. 6. A model of water binding to and release from the Mn cluster during the S-state transition cycle of PS II. The structure of Mn-cluster was drawn according to the PS II structure given by Loll et al. [8]. It is unknown yet whether Mn1 or Mn3 is oxidized in the transition from S_0 to S_1 states so that the oxidation of Mn3 is assumed tentatively in the transition from S_0 to S_1 states in this scheme. Note that the proton release and water oxidation have not been included in this scheme.

the manganese. Our results showed that the central region of the ENDOR spectra of S_0 and S_2 multiline signals partially decreased, which might be related to the protons at relatively long distances as detected by ^{2}H-ESEEM [43]. The slow exchange rates might represent the exchange of protons on the amino acid side-chains. On the other hand, pulsed ENDOR study showed that all these signals were exchangeable within 60 min [30], and simulation revealed a proton that interacts isotropically with the metal-bound proton [30], though these protons were not detected by CW-ENDOR. The differences might arise from the different ENDOR mechanisms of CW and pulsed ENDOR measurements. In principle, pulsed ENDOR gives no intensity for small hyperfine couplings, such as matrix lines, that are produced by the effect of "distant protons" [44,45]. Therefore, the changes of peak intensities in pulsed ENDOR are not necessarily caused by deuterium exchange of the observed protons.

Fig. 6 shows a schematic model for the S-state transitions and proton binding based on the present study. Although the ee′ protons detected in the S_0 and S_2 ENDOR spectra were tentatively assigned in this scheme as belonging to one water molecule, the number and chemical nature of the protons giving rise to this and the ff′ ENDOR signals are still unclear. As pointed out above, the ff′ proton(s) are unlikely to belong to substrate water, and are therefore represented by H_nX, where X is suggested to represent an amino acid ligand to Mn and n gives the number of exchangeable protons of this ligand. The S_0 state is assumed to contain Mn_4(III,III,III,IV) [15]. The numbering of manganese ions is based on the report given by Loll et al. [8], who suggested that Mn2 is oxidized from Mn(III) to Mn(IV) in the S_1–S_2 transition, based on the FTIR results [46,47], and Mn4 is not oxidized to Mn(IV) during the S state transitions. Mn1 or Mn3 is assumed to be Mn(III) or Mn(IV) in S_1 state. Then, Mn1 or Mn3 can be oxidized from Mn(III) to Mn(IV) in the S_0–S_1 transition. In this scheme, Mn3 is assumed to be the binding site of H_nX (ff′ protons) and that the exchange of the ff′ protons is slowed by the Mn(III) to Mn(IV) oxidation of Mn3 during the S_0 to S_1 transition. Hiller and Wydrzynski calculated that the exchange rate of oxygen belonging to water at a metal center decreases with oxidation of the metal center and the decrease in ionic radius, with an exchange rate of 10^{-6} to 10^{-4} s^{-1} for Mn(IV) and 10^{-2} to 10^{0} s^{-1} for Mn(III) [19]. We note that there is no simple correlation between Mn oxidation and the exchange rates of associated protons and that Mn oxidation may also lead to an increase of the proton exchange rates due to acidification depending on the type of exchange mechanism. Furthermore, we tentatively assume that the ee′ proton(s) belong to one substrate water molecule that binds to Mn1. The values of 2.7 and 3.3 Å for the ff′ and ee′ protons gives rough estimations of the distances between the protons and the spin center of the four manganese ions. These protons are, therefore, assumed to be located closer to each manganese atom and to change their affinities during the turnover of the S state. The effects of chemical or structural modifications such as proton release are also required to accurately define the site of binding protons.

Acknowledgments

The research was financially supported from Japanese Ministry of Education, Science, Sports and Culture by Grant-in-Aid for Scientific Research for Young Scientists (B) (17740222) to H.M. and Scientific Research (B) (17370055) to S.I. and by the 21st Century Center of Excellence program for "The origin of the universe and matter" (to S.I. and H.M.).

References

[1] B. Ke, The Photosynthesis: Photobiochemistry and Photobiophysics, Kluwer, The Netherlands, 2001.
[2] R.J. Debus, The manganese and calcium ions of photosynthetic oxygen evolution, Biochim. Biophys. Acta 1102 (1992) 269–352.
[3] V.K. Yachandra, K. Sauer, M.P. Klein, Manganese cluster in photosynthesis: where plants oxidize water to dioxygen, Chem. Rev. 96 (1996) 2927–2950.
[4] A. Zouni, H.T. Witt, J. Kern, P. Fromme, N. Krauss, W. Saenger, P. Orth, Crystal structure of photosystem II from *Synechococcus elongatus* at 3.8 Å resolution, Nature 409 (2001) 739–743.
[5] K.N. Ferreira, T.M. Iverson, K. Maghlaoui, J. Barber, S. Iwata, Architecture of the photosynthetic oxygen-evolving center, Science 303 (2004) 1831–1838.
[6] N. Kamiya, J.R. Shen, Crystal structure of oxygen-evolving photosystem II from *Thermosynechococcus vulcanus* at 3.7-Å resolution, Proc. Natl. Acad. Sci. U. S. A. 100 (2003) 98–103.
[7] J. Biesiadka, B. Loll, J. Kern, K.D. Irrgang, A. Zouni, Crystal structure of cyanobacterial photosystem II at 3.2 Å resolution: a closer look at the Mn-cluster, Phys. Chem. Chem. Phys. 6 (2004) 4733–4736.
[8] B. Loll, J. Kern, W. Saenger, A. Zouni, J. Biesiadka, Towards complete cofactor arrangement in the 3.0 Å resolution structure of photosystem II, Nature 438 (2005) 1040–1044.
[9] G.C. Dismukes, Y. Siderer, Intermediates of a polynuclear manganese center involved in photosynthetic oxidation of water, Proc. Natl. Acad. Sci. U. S. A. 78 (1981) 274–278.
[10] M. Zheng, G.C. Dismukes, Orbital configuration of the valence electrons, ligand field symmetry, and manganese oxidation states of the photosynthetic water oxidizing complex: analysis of the S2 state multiline EPR signals, Inorg. Chem. 35 (1996) 3307–3319.
[11] K.K. Hasegawa, M. Kusunoki, Y. Inoue, T.A. Ono, Simulation of S2-state multiline EPR signal in oriented photosystem II membranes: structural implications for the manganese cluster in an oxygen-evolving complex, Biochemistry 37 (1998) 9457–9465.
[12] K. Hasegawa, T. Ono, Y. Inoue, M. Kusunoki, How to evaluate the structure of a tetranuclear Mn cluster from magnetic and EXAFS data: case of the S2-state Mn-cluster in photosystem II, Bull. Chem. Soc. Jpn. 72 (1999) 1013–1023.
[13] K.V. Lakshmi, S.S. Eaton, G.R. Eaton, G.W. Brudvig, Orientation of the tetranuclear manganese cluster and tyrosine Z in the O_2-evolving complex of photosystem II: an EPR study of the S2Yz$^{\bullet}$ state in oriented acetate-inhibited photosystem II membranes, Biochemistry 38 (1999) 12758–12767.
[14] J.M. Peloquin, K.A. Campbell, D.W. Randall, M.A. Evanchik, V.L. Pecoraro, W.H. Armstrong, R.D. Britt, ^{55}Mn ENDOR of the S_2-state multiline EPR signal of photosystem II: implications on the structure of the tetranuclear Mn cluster, J. Am. Chem. Soc. 122 (2000) 10926–10942.
[15] L.V. Kulik, B. Epel, W. Lubitz, J. Messinger, ^{55}Mn pulse ENDOR at 34 GHz of the S_0 and S_2 states of the oxygen-evolving complex in photosystem II, J. Am. Chem. Soc. 127 (2005) 2392–2393.
[16] J. Messinger, J.H.A. Nugent, M.C.W. Evans, Detection of an EPR multiline signal for the S_0^* state in photosystem II, Biochemistry 36 (1997) 11055–11060.
[17] P. Geijer, S. Peterson, K.A. Åhrling, Z. Deak, S. Styring, Comparative studies of the S_0 and S_2 multiline electron paramagnetic resonance signals

from the manganese cluster in Photosystem II, Biochim. Biophys. Acta 1503 (2001) 83–95.
[18] J. Messinger, M. Badger, T. Wydrzynski, Detection of one slowly exchanging substrate water molecule in the S_3 state of photosystem II, Proc. Natl. Acad. Sci. U. S. A. 92 (1995) 3209–3213.
[19] W. Hillier, T. Wydrzynski, Oxygen ligand exchange at metal sites—Implications for the O_2 evolving mechanism of photosystem II, Biochim. Biophys. Acta 1503 (2001) 197–209.
[20] G. Hendry, T. Wydrzynski, The two substrate–water molecules are already bound to the oxygen-evolving complex in the S_2 state of photosystem II, Biochemistry 41 (2002) 13328–13334.
[21] W. Hillier, J. Messinger, Mechanism of photosynthetic oxygen production, in: T. Wydrzynski, K. Satoh (Eds.), Advances in Photosynthesis and Respiration, Photosystem II, vol. 22, Springer, Dordrecht, 2005, pp. 567–608.
[22] T. Noguchi, M. Sugiura, Flash-induced FTIR difference spectra of the water oxidizing complex in moderately hydrated photosystem II core films: effect of hydration extent on S-state transitions, Biochemistry 41 (2002) 2322–2330.
[23] T.J. Wydrzynski, S.B. Marks, P.G. Schmidt, Govindjee, H.S. Gutowsky, Nuclear magnetic-relaxation by manganese in aqueous suspensions of chloroplasts, Biochemistry 17 (1978) 2155–2162.
[24] T.J. Wydrzynski, Early indications for manganese oxidation state changes during photosynthetic oxygen production: a personal account, Photosynth. Res. 80 (2004) 125–135.
[25] A.N. Srinivasan, R.R. Sharp, Flash-induced enhancements in the proton NMR relaxation rate of Photosystem II particles, Biochim. Biophys. Acta 850 (1986) 211–217.
[26] A.N. Srinivasan, R.R. Sharp, Flash-induced enhancements in the proton NMR relaxation rate of photosystem II particles: response to flash trains of 1–5 flashes, Biochim. Biophys. Acta 851 (1986) 369–376.
[27] A. Kawamori, T. Inui, T. Ono, Y. Inoue, ENDOR study on the position of hydrogens close to the manganese cluster in S2 State of Photosystem II, FEBS Lett. 254 (1989) 219–224.
[28] X.S. Tang, M. Sivaraja, G.C. Dismukes, Protein and substrate coordination to the manganese cluster in the photosynthetic water oxidizing complex—^{15}N and ^{1}H ENDOR spectroscopy of the S_2 state multiline signal in the thermophilic cyanobacterium *Synechococcus elongatus*, J. Am. Chem. Soc. 115 (1993) 2382–2389.
[29] R. Fiege, W. Zweygart, R. Bittl, N. Adir, G. Renger, W. Lubitz, EPR and ENDOR studies of the water oxidizing complex of Photosystem II, Photosynth. Res. 48 (1996) 227–237.
[30] C.P. Aznar, R.D. Britt, Simulations of the ^{1}H electron spin echo-electron nuclear double resonance and ^{2}H electron spin echo envelope modulation spectra of exchangeable hydrogen nuclei coupled to the S_2-state photosystem II manganese cluster, Phil. Trans. R. Soc. Lond. B 357 (2002) 1359–1365.
[31] R.D. Britt, K.A. Campbell, J.M. Peloquin, M.L. Gilchrist, C.P. Aznar, M.M. Dicus, J. Robblee, J. Messinger, Recent pulsed EPR studies of the Photosystem II oxygen-evolving complex: implications as to water oxidation mechanisms, Biochim. Biophys. Acta 1655 (2004) 158–171.
[32] D.A. Berthold, G.T. Babcock, C.F. Yocum, A highly resolved, oxygen-evolving photosystem-II preparation from spinach thylakoid membranes EPR and electron-transport properties, FEBS Lett. 134 (1981) 231–234.
[33] T. Ono, Y. Inoue, Effects of removal and reconstitution of the extrinsic 33, 24 and 16 kDa proteins on flash oxygen yield in photosystem II particles, Biochim. Biophys. Acta 850 (1986) 380–389.
[34] S. Styring, A.W. Rutherford, In the oxygen-evolving complex of photosystem-II the S_0 state is oxidized to the S_1 state by D^+ (Signal II_{slow}), Biochemistry 26 (1987) 2401–2405.
[35] J. Messinger, J.H. Robblee, W.O. Yu, K. Sauer, V.K. Yachandra, M.P. Klein, The S_0 state of the oxygen-evolving complex in photosystem II is paramagnetic: detection of an EPR multiline signal, J. Am. Chem. Soc. 119 (1997) 11349–11350.
[36] K.A. Åhrling, S. Peterson, S. Styring, An oscillating manganese electron paramagnetic resonance signal from the S0 state of the oxygen evolving complex in photosystem II, Biochemistry 36 (1997) 13148–13152.
[37] L. Kulik, B. Epel, J. Messinger, W. Lubitz, Pulse EPR, ^{55}Mn-ENDOR and ELDOR-detected NMR of the S_2-state of the oxygen evolving complex in Photosystem II, Photosynth. Res. 84 (2005) 347–353.
[38] E. Schlodder, H.T. Witt, Stoichiometry of proton release from the catalytic center in photosynthetic water oxidation, J Biol. Chem. 274 (1999) 30387–30392.
[39] M. Haumann, W. Junge, Protons and charge indicators in oxygen evolution, in: D.R. Ort, C.F. Yocum (Eds.), Oxygenic Photosynthesis: The Light Reactions, The Netherland, Dordrecht, 1996, pp. 165–192.
[40] J.H.A. Nugent, A.M. Rich, M.C.W. Evans, Photosynthetic water oxidation: towards a mechanism, Biochim. Biophys. Acta 1503 (2001) 138–146.
[41] W. Hillier, T. Wydrzynski, The affinities for the two substrate water binding sites in the O_2 evolving complex of photosystem II vary independently during S-state turnover, Biochemistry 39 (2000) 4399–4405.
[42] W. Hillier, T. Wydrzynski, Substrate water interactions within the Photosystem II oxygen evolving complex, Phys. Chem. Chem. Phys. 6 (2004) 4882–4889.
[43] M.C.W. Evans, A.M. Rich, J.H.A. Nugent, Evidence for the presence of a component of the Mn complex of the photosystem II reaction centre which is exposed to water in the S_2 state of the water oxidation complex, FEBS Lett. 477 (2000) 113–117.
[44] G. Schweiger, G. Jeschke, Principles of Pulsed Electron Paramagnetic Resonance, Oxford University Press, Inc., New York, 2001, pp. 389–405.
[45] A.V. Astashkin, A. Kawamori, Matrix line in pulsed electron-nuclear double resonance spectra, J. Magn. Reson. 135 (1998) 406–417.
[46] Y. Kimura, N. Mizusawa, T. Yamanari, A. Ishii, T. Ono, Structural changes of D1 C-terminal α-carboxylate during S-state cycling in photosynthetic oxygen evolution, J. Biol. Chem. 280 (2005) 2078–2083.
[47] R.J. Debus, M.A. Strickler, L.M. Walker, W. Hillier, No evidence from FTIR difference spectroscopy that aspartate-170 of the D1 polypeptide ligates a manganese ion that undergoes oxidation during the S_0 to S_1, S_1 to S_2, or S_2 to S_3 transitions in photosystem II, Biochemistry 44 (2005) 1367–1374.